^{18}F-NaF imaging of vulnerable plaques and myocardial scar tissue using hybrid PET/CT and PET/MRI

By Dr Stephanie Marchesseau

This review summarizes recently published findings that confirmed the role of ^{18}F-NaF PET/CT in the imaging of culprit coronary atheromata while demonstrating for the first time the potential of ^{18}F-NaF PET/MRI to identify infarcted myocardium [1].

INTRODUCTION

Rupture or erosion of coronary lesions results in sudden occlusion of major arteries causing acute myocardial infarction (AMI), which is a major cause of cardiac death or disability worldwide and is extremely difficult to predict.

Invasive imaging techniques to detect vulnerable plaques are still the gold standard methodology but the medical community is increasingly recognizing that mere identification of these lesions is not sufficient as many of them are in fact stable. A more efficient approach would be to detect active plaques prone to rupture as their presence in itself indicates an increased risk of myocardial infarction. Recently, non-invasive PET/CT imaging using ^{18}F-NaF has shown the potential to identify high-risk plaques [2, 3] and has become a research focus in coronary imaging.

From these findings, it is currently clear that ^{18}F-NaF targets active coronary plaques but it remains uncertain what is the mechanism involved and whether ^{18}F-NaF has other potential roles in cardiac imaging. PET/CT studies in a rat model indicated that ^{18}F-NaF may possibly target apoptosis [4]. Histological analyses of carotid artery plaques suggested that ^{18}F-NaF targeted macrophage infiltration and necrosis [5]. As prior studies have shown varying degrees of calcification in previously infarcted myocardium, we hypothesized that ^{18}F-NaF could also detect scar tissue arising from myocardial infarction [1]. We therefore sought first to independently validate the use of ^{18}F-NaF PET/CT imaging for the detection of high-risk coronary lesions. Using ^{18}F-NaF PET/MR imaging, we then intended to quantify the uptake of ^{18}F-NaF in myocardial scar tissue relative to remote healthy myocardium to gain further knowledge of the processes common to infarction and atheromata.

The Author

Dr Stephanie Marchesseau

Clinical Imaging Research Centre,

A*STAR-NUS, Singapore,

Singapore

email: marchesseau.stephanie@gmail.com

STUDY DESIGN

Ten patients presenting with ST-Elevation Myocardial Infarction (STEMI) were enrolled in this study. All patients had an acute occlusion of an infarct-related artery (IRA) on coronary angiography and underwent emergency PCI with stent placement within 12 hours of symptom onset. After PCI, consented patients were screened for eligibility and were then scanned 15 days after the acute event by PET/MRI for 75 minutes and a few minutes later by PET/CT for 10 minutes [protocol shown in Figure 1]. PET uptake was measured using Standardized Uptake Value (SUV).

Angiography examination:

All patients underwent manual thrombectomy, balloon angioplasty and coronary stent implantation as directed by the primary clinician operator within 6 hours of the acute event. Culprit plaques were spatially defined by the presence of an occlusive or subocclusive lesion within the IRA corresponding to echocardiographic localization. Culprit lesions on coronary angiography were then mapped to corresponding calcium regions on the CT image and each calcium region assigned a culprit or non-culprit label [Figure 2B].

PET/MR imaging for myocardial infarct uptake

All subjects were first scanned on a Biograph mMR PET/MR scanner (Siemens Healthineers, Erlangen, Germany) for 75 minutes. MRI and PET scans were performed simultaneously on a single bed centered over the heart. The PET/MRI

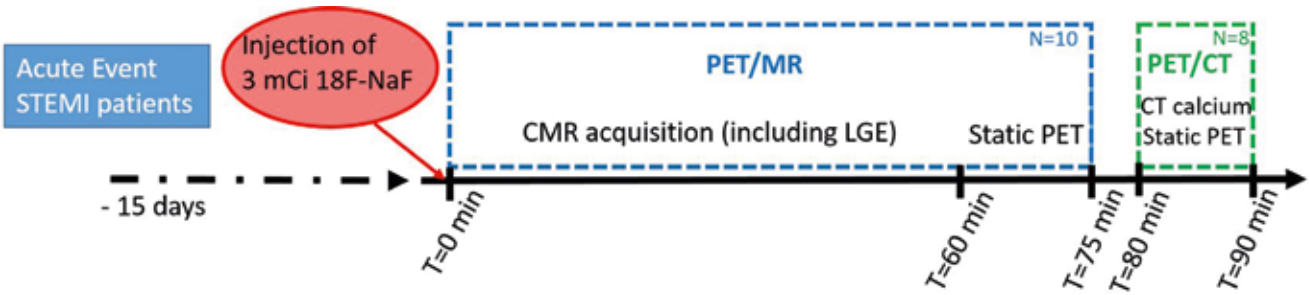

FIGURE 1. Representation of the study imaging protocol

scan was started immediately after intravenous injection of 2.95 +/- 0.21 mCi ^{18}F-NaF. PET data were reconstructed from the last 15 minutes without ECG or respiratory gating. A standard Cardiovascular Magnetic Resonance (CMR) protocol was used for image acquisition, simultaneously including CINE steady state free precession and Late Gadolinium enhancement (LGE) short axis images.

After co-registration with the PET image (when necessary), scar regions and healthy remote myocardium were extracted from manual delineation on the LGE images and SUV reported for these regions. The Tissue-to-background ratio (TBR) in the myocardium was measured as the mean SUV within the ROI (scar or remote myocardium) divided by the mean SUV within the left ventricle blood pool away from the walls.

PET/CT imaging for coronary atheromata uptake

Of the 10 subjects who underwent PET/MR scanning, eight subjects were then immediately transferred to a Biograph mCT PET/CT scanner (Siemens Healthineers, Erlangen, Germany) for a non-enhanced coronary artery calcium score CT scan immediately followed by a 10 min PET scan (one bed position centered over the heart).

Calcium regions within the arteries were delineated manually on the 3D CT image [Figure 2C] as well as each vessel containing at least one calcium region. Hybrid PET/CT acquisition ensures the direct transposition of these Regions of Interest (ROIs) on the PET image [Figure 2D], thereby enabling the automatic measurement of SUV within each region. The TBR of each calcium ROI, as validated by Josh *et al.*[5], was then measured as the ratio between the calcium region maximum SUV over the corresponding vessel mean SUV.

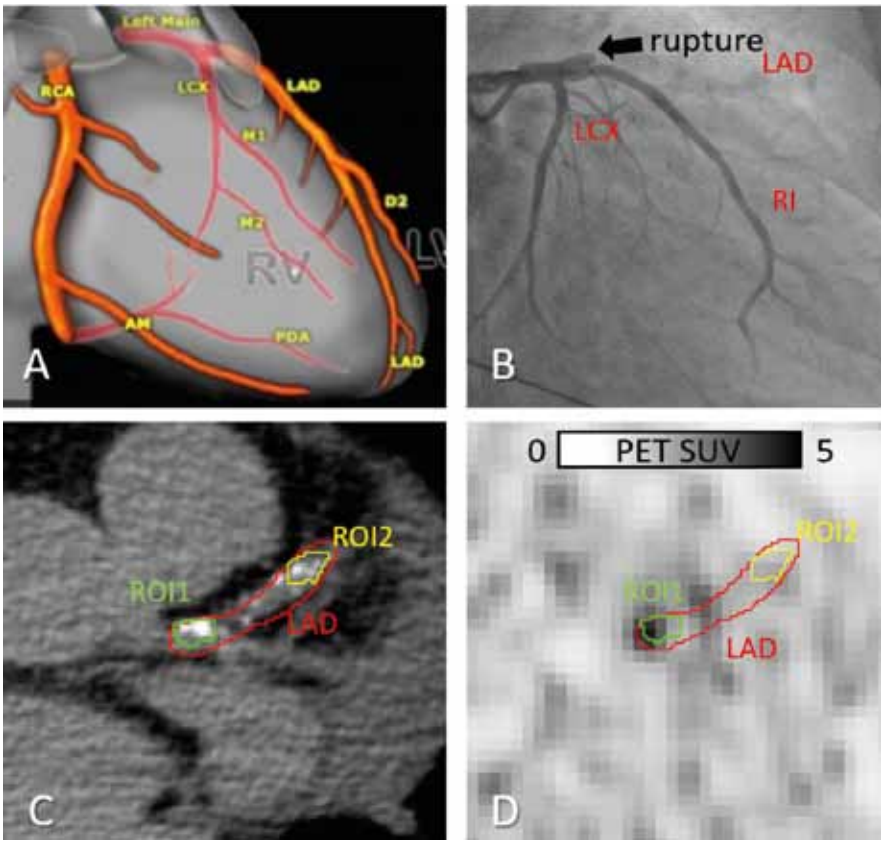

FIGURE 2. A) Definition of the coronary arteries. B) Angiogram image showing plaque rupture and acute occlusion at proximal LAD. C) CT calcium image showing two lesions in LAD. D) PET image showing higher uptake in ROI1.

RESULTS

Coronary atheromata imaging

Visual distinction of vulnerable plaques on the PET image was highly challenging due to the small size of the plaques, the limited resolution of the PET image, as well as respiratory and cardiac motion, leading to large partial volume effect. In the example shown in Figure 2, the culprit (high risk) plaque as assessed by angiography is ROI 1 while ROI 2 was diagnosed as a low risk plaque. On the PET image, a visual difference in uptake between the two ROIs is noticeable, despite the high level of surrounding noise. This non-specific uptake renders the detection of vulnerable plaques impossible if SUVs of plaques are compared without normalization to background.

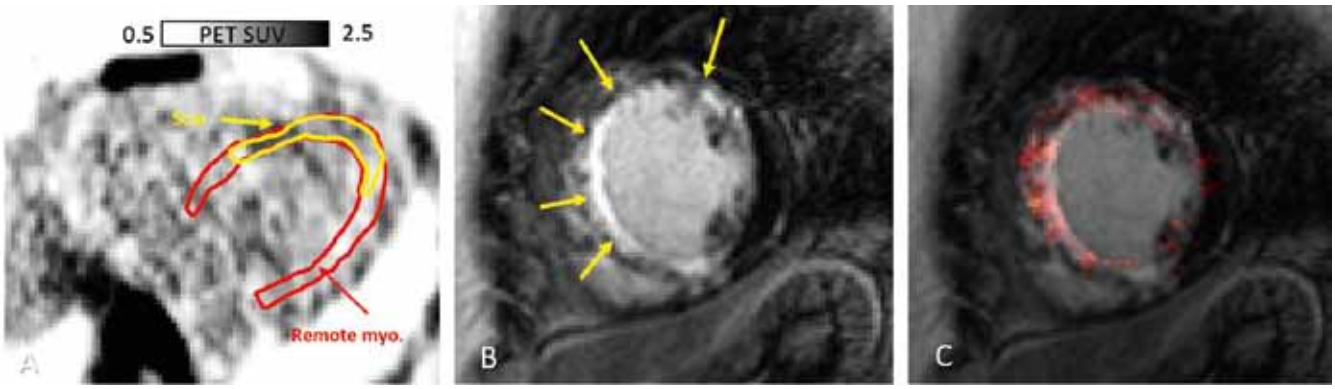

FIGURE 3. A) PET image with overlaid scar and myocardium regions showing higher uptake in scar despite amount of noise. B) Example short-axis LGE image (yellow arrows pointing to scar tissue). C) Same LGE image fused with PET image masked to the myocardium segmentation showing higher but non-uniform uptake within the scar tissue.

Of the 33 lesions detected on CT, 8 were identified as being culprit on the standard coronary angiogram, one for each patient undergoing PET/CT. The TBR of the culprit lesions was found to be significantly higher than that of non-culprit lesions with an average value of 2.11 for culprit (±0.42) vs. 1.36 (±0.30) for non-culprit (p-value < 0.001, d=1.77), which is consistent with previously published studies.

Myocardial scar imaging

Visual distinction of scar tissue on the PET/MR image was as challenging as for the atheromata. An example is shown Figure 3A in which most parts of the scar have higher uptake than the average myocardium. However, partial volume effects, breathing and beating of the heart reduce the uptake to a low value. One can also notice that the uptake in the blood pool is globally higher than in the myocardium. Once again the uptake is not specific to the scar and a similar uptake is observed in the turbulent blood pool or surrounding tissue. Moreover, uptake in scar tissue was found to be inhomogeneous suggesting that various processes occur during scar formation [Figure 3C].

Nine of the 10 patients had clear visible zones of scar tissue defined on the LGE image. The TBR was found to be significantly higher in scar tissue than in the remote healthy myocardium, with an average value of 0.81 (±0.10) for scar tissue compared to 0.72 (±0.06) for remote myocardium (p-value=0.03, d=1.55).

DISCUSSION

To conclude, the study described more fully in [1] first confirms previous findings of successful differentiation of high-risk coronary atheromata in the IRA of patients with recent STEMI using ^{18}F-NaF PET/CT non-invasive imaging. This proves once more the potential of such an approach to differentiate between high and low risk atheromata and therefore predict high-risk patients. However, the quality of the images acquired in this study demonstrate that further research is required before ^{18}FNaF PET imaging can be used as a routine diagnostic tool. In addition, further validation is needed in order to establish a reliable PET threshold to define a high-risk plaque.

For the first time in humans, simultaneous ^{18}F-NaF uptake was observed using LGE and PET/MR in myocardial scar in the area supplied by the IRA. Despite spillage from the left ventricular blood pool that could affect the SUV, partial volume effects due to respiratory and cardiac motion, and potential misregistration between PET/MR and LGE, we demonstrated that ^{18}F-NaF is taken up by both culprit coronary atheromata and myocardial scar tissue.

The reasons why ^{18}F-NaF binds to ruptured or vulnerable plaque are still unknown. In recent studies, Irkle *et al* [6]. differentiated stable macrocalcification from high risk microcalcification to explain the preferred binding of ^{18}F-NaF to culprit plaques. Increased uptake of calcium could also be due to retention of calcific deposits in the extracellular space present due to myocyte necrosis [7]. Without histological analysis, it is impossible to determine with certainty the common processes between myocardial infarct and culprit lesion uptake at this stage. We hypothesize nonetheless that many of the cell death mechanisms in atherosclerotic plaque disruption are common to myocardium infarction. This study finally serves as a proof-of-concept that ^{18}FNaF PET/CT imaging could potentially be used as a unique technique to quantify both vulnerable plaque burden and myocardial scar tissue simultaneously.

REFERENCES

1. Marchesseau S, *et al.* Hybrid PET/CT and PET/MRI imaging of vulnerable coronary plaque and myocardial scar tissue in acute myocardial infarction. Journal of Nuclear Cardiology, 2017 May: p 1-11.
2. Dweck MR *et al.* Assessment of valvular calcification and inflammation by positron emission tomography in patients with aortic stenosis. Circulation, 2012; 125: 76.
3. Dweck MR *et al.* Coronary arterial ^{18}F-sodium fluoride uptake: a novel marker of plaque biology. Journal of the American College of Cardiology, 2012; 59: 1539.
4. Han JH *et al.* Sodium [^{18}F] Fluoride PET/CT in Myocardial Infarction. Molecular Imaging and Biology. 2015; 17: 214.
5. Joshi NV *et al.* 18 F-fluoride positron emission tomography for identification of ruptured and high-risk coronary atherosclerotic plaques: a prospective clinical trial. The Lancet, 2014; 383: 705.
6. Irkle A *et al.* Identifying active vascular microcalcification by ^{18}F-sodium fluoride positron emission tomography. Nature Communications, 2015; 6: 7495.
7. Dongworth RK *et al.* Targeting mitochondria for cardioprotection: examining the benefit for patients. Future Cardiology, 2014; 10: 255.